Biochimica et Biophysica Acta 1830 (2013) 2204–2213

Contents lists available at SciVerse ScienceDirect

Biochimica et Biophysica Acta

journal homepage: www.elsevier.com/locate/bbagen

CHK1 cleavage in programmed cell death is intricately regulated by both caspase and non-caspase family proteases

Naoyuki Okita [a,*], Miyuki Yoshimura [b], Kazuhito Watanabe [a], Shota Minato [a], Yuki Kudo [b], Yoshikazu Higami [a], Sei-ichi Tanuma [b]

[a] Department of Molecular Pathology and Metabolic Disease, Tokyo University of Science, 2641 Yamazaki, Noda-shi, Chiba 278-0022, Japan
[b] Department of Biochemistry, Faculty of Pharmaceutical Sciences, Tokyo University of Science, 2641 Yamazaki, Noda-shi, Chiba 278-0022, Japan

ARTICLE INFO

Article history:
Received 10 April 2012
Received in revised form 18 September 2012
Accepted 10 October 2012
Available online 16 October 2012

Keywords:
CHK1
DNA damage response
Programmed cell death
Caspase family proteases
Non-caspase family proteases

ABSTRACT

Background: CHK1 is an important effector kinase that regulates the cell cycle checkpoint. Previously, we showed that CHK1 is cleaved in a caspase (CASP)-dependent manner during DNA damage-induced programmed cell death (PCD) and have examined its physiological roles.
Methods and results: In this study, we investigated the behavior of CHK1 in PCD. Firstly, we found that CHK1 is cleaved at three sites in PCD, and all cleavages were inhibited by the co-treatment of a pan-CASP inhibitor or serine protease inhibitors. We also showed that CHK1 is cleaved by CASP3 and/or CASP7 recognizing at ^{296}SNLD^{299} and ^{348}TCPD^{351}, and that the cleavage results in the enhancement of CHK1 kinase activity. Furthermore, as a result of the characterization of cleavage sites by site-directed mutagenesis and an analysis performed using deletion mutants, we identified ^{320}EPRT^{323} as an additional cleavage recognition sequence. Considering the consensus sequence cleaved by CASP, it is likely that CHK1 is cleaved by non-CASP family protease(s) recognizing at ^{320}EPRT^{323}. Additionally, the cleavage catalyzed by the ^{320}EPRT^{323} protease(s) markedly and specifically increased when U2OS cells synchronized into G1 phase were induced to PCD by cisplatin treatment.
Conclusion: CHK1 cleavage is directly and indirectly regulated by CASP and non-CASP family proteases including serine protease(s) and the "^{320}EPRT^{323} protease(s)." Furthermore, ^{320}EPRT^{323} cleavage of CHK1 occurs efficiently in PCD which is induced at the G1 phase by DNA damage.
General significance: CASP and non-CASP family proteases intricately regulate cleavage for up-regulation of CHK1 kinase activity during PCD.

1. Introduction

DNA damage induced by anti-cancer drugs, ultraviolet light and ionizing radiation compromises the maintenance of genomic integrity. Cells of multicellular organisms harbor two major pathways to protect from DNA damage. DNA repair initiated at the cell cycle checkpoint is the initially responsive protective machinery and contributes to cell survival. Programmed cell death (PCD) provides a further response to protect against DNA damage. Failure of these mechanisms threatens the survival of individual organisms via aberrant cell survival and cancer progression. One of the signature apoptotic mechanisms is cleavage of various cellular proteins by the caspase (CASP) family [1,2]. Within the CASP family, CASP2, CASP3, CASP6, CASP7, CASP8, CASP9, and CASP10 are categorized as apoptotic CASPs, which orchestrate the apoptotic cascade [1–5]. Although all CASPs including inflammatory CASPs display preferential recognition, it is required that the P1 residue, which is the site of cleavage, is an aspartic acid [3–5]. The involvements of non-CASP family proteases including certain serine proteases, calpains and lysosomal proteases in various modes of PCD including apoptotic cell death have also been reported [6]. These findings have suggested that apoptotic protease is not only CASP family protease. However, it remains unclear whether these non-CASP family proteases regulate apoptotic cell death directly or indirectly (for example, via other modes of PCD). Taken together, protein cleavage by proteases may be a common regulatory mechanism of various modes of PCD.

Regulatory factors in DNA damage response such as PARP1, RAD51, ATM, RAD9, CLASPIN, CHK1, and MDC1 have been reported as "death substrates" cleaved by apoptotic CASPs in PCD [7–13]. On the other hand, it has been less reported about cleavage of proteins involved in DNA damage by non-CASP family proteases. Since DNA damage response consists of various physiological processes (for example, DNA damage recognition, DNA repair, and cell cycle checkpoint etc.), it is important to understand the mechanisms and roles of the cleaved proteins in PCD regulation. Furthermore, one unresolved question in DNA damage-induced PCD concerns whether the PCD

* Corresponding author at: Department of Molecular Pathology and Metabolism, Faculty of Pharmaceutical Sciences, Tokyo University of Science, 2641 Yamazaki, Noda-shi, Chiba 278-0022, Japan. Tel./fax: +81 4 7121 3676.
E-mail addresses: nokita7@rs.noda.tus.ac.jp, nmsokita@gmail.com (N. Okita).

0304-4165/$ – see front matter © 2012 Elsevier B.V. All rights reserved.
http://dx.doi.org/10.1016/j.bbagen.2012.10.009

regulation at each cell cycle phase is identical. For example, mitotic catastrophe is one of the PCD pathways induced at M phase [1,2]. While CASP activation is observed during mitotic catastrophe, the regulation mechanism is not always identical to apoptotic cell death [1,2]. Furthermore it was shown that mitotic catastrophe executes in cell death by CASP-dependent and -independent mechanisms [14]. While scientific evidence with regard to cell cycle-specific PCD has been little shown, these findings with regard to mitotic catastrophe suggests the existence of cell cycle-selective PCD pathways.

We have previously investigated the mechanism of DNA damage-induced PCD and discovered that CHK1, an important effector kinase that regulates the cell cycle checkpoint, is cleaved in a CASP-dependent manner during etoposide-induced PCD [12]. Another group subsequently demonstrated that the CASP cleavage sites of CHK1 are D^{299} and D^{351} [15]. Furthermore, it was recently reported that the CHK1 signaling pathway controls PCD [16,17]. These findings indicate that CHK1 may be one of the key molecules that link the checkpoint to PCD. In this study, we focus on the behavior of CHK1 in DNA damage-induced PCD and demonstrate the involvements of CASP and non-CASP family proteases in CHK1 cleavage. Our results suggest that CHK1 cleavage is intricately regulated during DNA damage-induced PCD and provide a good model of dual regulation by CASP and non-CASP family proteases.

2. Materials and methods

2.1. Cells and drugs

U2OS and HeLaS3 cells were maintained in DMEM (WAKO, Osaka, Japan) supplemented with 10% fetal calf serum (BOVOGEN, East Keilor, VIC, Australia) and 1% penicillin/streptomycin (SIGMA, St. Louis, MO, USA). For immunocytochemistry, cells were seeded on poly-D-lysine-coated glass coverslips and subsequently treated. Anti-Fas (clone CH11) was supplied by MBL (Aichi, Japan). Benzyloxycarbonyl-Val-Ala-Asp (OMe) fluoromethylketone (z-VAD-fmk) and *N*-carbobenzoxyl-L-leucinyl-L-leucinyl-L-norvalinal (LLnV) were from Peptide Institute (Osaka, Japan). *N*-Acetyl-L-leucyl-L-leucyl-L-norleucinal (LLnL) was purchased from Merck (Darmstadt, Germany). All other drugs were purchased from WAKO.

2.2. Western blotting

Cells were lyzed by the addition of lysis buffer (50 mM Tris–HCl pH 6.8, 2% SDS, 5% glycerol), boiled for 5 min, and sonicated. Protein concentrations of the soluble fraction were determined by the BCA protein assay (Thermo Fisher Scientific, Rockford, IL, USA) according to the manufacturer's protocol, and standardized by the addition of lysis buffer. 2-ME (5%) and bromophenol blue (0.025%) were subsequently added to protein solutions and the mixtures were boiled for 5 min. Equal amounts of proteins (5–20 μg) were subjected to SDS-PAGE and transferred to nitrocellulose membranes. The membranes were blocked with 2.5% skim milk and 0.25% BSA in TBS (50 mM Tris, pH 7.4, 150 mM NaCl) containing 0.1% Tween 20 (TTBS) for 1 h at room temperature, and probed with the appropriate primary antibodies overnight at 4 °C or for 2 h at room temperature. After washes with TTBS, the membranes were incubated with the appropriate secondary antibody, horseradish peroxidase-conjugated F(ab')2 fragment of goat anti-mouse IgG, anti-rabbit IgG, or anti-rat IgG (Jackson Immunoresearch Laboratories, West Grove, PA, USA), for 1 h at room temperature. After washing the membrane with TTBS, the membranes were incubated with ImmunoStar LD reagent (WAKO). The specific proteins were visualized with LAS3000 (FUJI FILM, Tokyo, Japan), and the data were analyzed using MultiGauge software (FUJI FILM).

2.3. Antibodies

As primary antibodies, anti-β-actin (clone AC-15, SIGMA, USA), anti-CASP-3 (clone 1F3, MBL, Japan), anti-CASP-7 (Cell Signaling Technology, USA), anti-CASP-9 (Cell Signaling Technology, USA), anti-CHK1 N-ter (clone DCS-310, MBL, Japan), anti-CHK1 C-ter (clone EP691Y, Epitomics, USA), anti-Cyclin D1 (clone DCS-6, MBL, Japan), anti-HTRA2 (clone 18-1-83, MBL, Japan), anti-MPM2 (clone MPM-2, Millipore, USA), anti-Myc (clone PL14, MBL, Japan), and anti-Parp1 (clone C-2-10, WAKO, Japan) antibodies were used.

2.4. Site-directed mutagenesis

Site-directed mutagenesis was performed by an overlap extension method using pcDNA-FLAG-CHK1wtsm-MycHis as a template DNA. Overlap extension reaction (15 μL) was performed using 1.5 unit Accuprime Pfx polymerase (Invitrogen), 200 ng template DNA, and 4.5 pmol each forward and reverse primers under the following conditions: initiation step, 94 °C for 3 min; cycling steps, 25 cycles of at 94 °C for 1 min, at 55 °C for 30 s, at 68 °C for 4.5 min; termination step, at 68 °C for 4.5 min. After incubation at 98 °C for 1 min, the reaction product was slowly cooled down to room temperature. For digestion of template DNA, the reaction product was treated with 20 unit Dpn I (New England Biolabs, UK) at 37 °C for 2 h and was directly used for transformation.

2.5. Construction of various CHK1 vectors

For CHK1 cleavage mutant vectors, CHK1 mutant cDNA digested from the pcDNA-FLAG-hCHK1 mutant sm-MycHis by *Hin*dIII and *Pme*I was cloned into the same sites of pIRES2-EGFP. For tetracycline-inducible recombinant CHK1 expression vectors, CHK1sm cDNA was amplified by PCR using Kozak-3FLAG-CHK1-F and 3Myc CHK1-R primers. After phosphorylation of the 5′ ends by T4 polynucleotide kinase (TaKaRa), the cDNA fragment was cloned into EcoRV-digested pTRE2-hyg. For CHK1 deletion mutant expression vectors, cDNAs of C- or N-terminal deletion CHK1 mutant containing 3× Myc tag were constructed via two steps of PCR. In the first step, a DNA fragment coding a deletion mutant was amplified by PCR using phCHK1smD299E-IRES2-EGFP or phCHK1smD351E-IRES2-EGFP (as a DNA template), a forward primer for deletion mutant, and a reverse primer (kozak-CHK1-F for C-terminal deletion or CHK1-R for N-terminal deletion). In the second step, a deletion mutant cDNA fragment containing 3× Myc tag sequence was amplified by PCR using a DNA fragment amplified in the first step (as a DNA template) and a primer set (kozak-CHK1-F and 3Myc-R for C-terminal deletion or kozak-ATG-3Myc-F and CHK1-R for N-terminal deletion). After phosphorylation of the 5′ ends by T4 polynucleotide kinase, the cDNA fragment was cloned into *Sma*I-digested pIRES2-EGFP. The primer sequences for deletion mutants or point mutants used were listed in Supplemental Table SI or SII, respectively.

2.6. Preparation of recombinant CHK1

U2OS tet-on cells (Clontech, Japan) were transfected with *Nru*I-linearized pTRE2-hyg vectors containing 3× FLAG-CHK1(WT)–3× Myc, 3× FLAG-CHK1(D299E)–3× Myc, or 3× FLAG-CHK1(D351E)–3× Myc cDNA using Fugene HD (Promega, USA) according to the manufacture's protocol. Each stable transfectant was selected with 600 μg/mL hygromycin B. Established U2OS tet-on/Chk1 cells were maintained in DMEM containing 10% FCS, 1% penicillin-streptomycin solution, 120 μg/mL hygromaycin B, and 200 μg/mL G418. For induction of recombinant CHK1s, U2OS tet-on/Chk1 cells were grown in the presence of 5 μg/mL of doxycycline for 2 days. The recombinant CHK1s were purified with anti-FLAG beads (SIGMA) and anti-Myc beads (MBL).

2.7. Production of recombinant CASPs

6× His-tagged active CASPs were prepared with recombinant protein expression methods using pET system, with minor modifications, as described in elsewhere [4]. CASP2 and the other CASPs were fused 6× His tag at the N-terminus and the C-terminus, respectively. The expressed active CASPs were purified with TALON resin (Clontech).

2.8. CASP cleavage assay

Recombinant active CASP2, CASP3, CASP6, CASP7, CASP8, CASP9, and CASP10 were obtained as described in the supplemental information. Recombinant CHK1 was incubated with each recombinant CASP in CASP assay buffer (20 mM HEPES–NaOH, pH 7.4, 15 mM $MgCl_2$, 0.01% Nonidet-P40, 5% glycerol, 10 mM DTT) at 37 °C for 8 or 24 h. For Western blotting analysis of cleavage profile, the reaction was stopped by the addition of SDS sample buffer. For kinase activity analysis, aliquots of reaction mixture were subjected to CHK1 kinase assays.

2.9. CHK1 kinase assay

Recombinant GST-CDC25C fragment was expressed and purified as described elsewhere [18]. Recombinant CHK1 was incubated with GST-CDC25C fragments at 37 °C for 30 min, and the reaction was stopped by the addition of SDS sample buffer. The kinase activity was visualized using Western blotting and quantified by chemiluminescense.

2.10. Cell synchronization and flow cytometry

For cell cycle synchronization, double thymidine block (DTB) or thymidine nocodazole block (TNB) methods were performed. For DTB, U2OS cells were seeded at 1.6×10^4 cells/cm^2. The next day, for the first synchronization, cells were treated with 2 mM thymidine for 21 h. For second synchronization, cells were incubated for a further 12 h in growth medium without thymidine, and treated with 2 mM thymidine and 12.5 μM deoxycytidine for 15 h. The G1/S synchronized cells were then released into growth medium. S or G2 phase-enriched cells were obtained at 4.5 or 8 h from release, respectively. For G1 phase-enriched cells, M phase cells obtained by release for 11 h followed by shake-off method were cultured in growth medium for 6 h. For TNB, U2OS cells were seeded at 1.6×10^4 cells/cm^2. The next day, for first synchronization, cells were treated with 2 mM thymidine for 21 h. After incubation for 6 h in growth medium without thymidine, for second synchronization the cells were treated with 200 nM nocodazole for 6 h. The mitosis-arrested cells obtained by the shake-off method were re-seeded at 1 to 2×10^4 cells/cm^2 for G1- or S-phase synchronization. G1 or S phase-enriched cells were obtained at 6 or 12 h from release, respectively. The cell cycle distribution was confirmed by flow cytometric analysis using propidium iodide (PI) staining as described below. Harvested cells were suspended in PBS and fixed with 70% ethanol at −20 °C overnight. The fixed cells were treated with 50 μg/mL PI and 200 μg/mL RNaseA at RT for 30 min, and were then analyzed by a FACS LSR flow cytometer (BD Biosciences, San Jose, CA, USA). Cell cycle data analysis was performed with CellQuest software (BD Biosciences).

2.11. RNAi

RNAi was performed using lipofectamine RNAiMAX reagent (Invitrogen, Carlsberg, CA, USA) according to the manufacture's protocol. Stealth siRNAs were purchased from Invitrogen. The target sequences were as follows: CASP3, ATAGAACCACTATGAAGCTACCTCA: CASP7, GGGTGAATGACAGAGTTGCCAGGCA: HTRA2, GGGAGGTGATTGGAGTG AACACCAT: Scramble (eGFP), CCAACUUGUCUGGUGUCAAAAAUAA.

3. Results

3.1. CHK1 cleavage in PCD and the involvement of CASP and serine protease families.

We previously demonstrated that CHK1 is cleaved during DNA damage-induced PCD in HeLa S3 cells [12]. This phenomenon appeared to be regulated by a CASP-dependent pathway, because a pan-caspase inhibitor, z-VAD-fmk, abolished CHK1 cleavage during DNA damage-induced PCD. In this study, we sought to perform further analysis of CHK1 cleavage during PCD. We treated U2OS cells with either etoposide (Etp) or cisplatin (Cis), at two different dosage levels, to induce moderate (cell viable) or severe (cell nonviable) DNA damage. The moderate and severe doses both induced DNA damage responses such as with CHK1 and H2AX phosphorylation (data not shown) in a dose-dependent manner. In cell lysates treated with higher doses, we detected several cleavage products with lower molecular weights than that of full-length CHK1. Interestingly, CHK1 was efficiently cleaved during DNA damage-induced PCD such as with Cis, camptothecin (Cpt) and Etp (Fig. 1B). The molecular weights of the products recognized by anti-CHK1 C-ter were approximately 15, 17 and 20 kDa (termed C1, C2, and C3, respectively) and those of products recognized by anti-CHK1 N-ter were approximately 42, 40 and 37 kDa (termed N1, N2, and N3). Considering that the molecular weight of full-length CHK1 is approximately 57 kDa, it is likely that N3–C3 and N1–C1 are cleavage products at D^{299} and D^{351}, respectively [15], and N2–C2 are from the unknown recognition sequence that is located between D^{299} and D^{351}. Our estimation of this combination was also supported by the product composition: in Cis treatment, C3 = C2 > C1 and N3 = N2 > N1; in Cpt treatment, C3 > C1 > C2 and N3 > N1 > N2; and in Etp treatment, C3 > C1 > C2 and N3 > N1 > N2. To confirm whether CHK1 cleavage is efficiently induced only by DNA damage-induced PCD, we further explored and then found that CHK1 cleavage efficiently occurs in LLnV- or LLnL-induced PCD (Fig. 1C). LLnV (also called MG115) and LLnL (also called MG101) are useful tools to examine the involvement of calpains, cathepsins, or proteasomes on an intracellular signaling pathway because both drugs are potent cell permeable inhibitors of calpains, cathepsins, or proteasomes [19]. Treatment with z-VAD-fmk also inhibited Etp, LLnV, or LLnL-induced CHK1 cleavage (Fig. 1C). As shown in Supplemental Fig. I, in HeLaS3 cells, all cleavages in Etp-induced PCD were inhibited by co-treatment with z-VAD-fmk. These results indicate that CHK1 cleavage occurs efficiently in DNA damage-induced PCD and certain types of protease inhibitor-induced PCD. Since it has been reported that PCD signals activate a certain type of serine protease such as HTRA2, AP24, and Cathepsin G [6,20–22], we examined the effects of some serine protease inhibitors, AEBSF, TLCK, or TPCK, on the CHK1 cleavage. As shown in Fig. 1D, all serine protease inhibitors we used inhibited the CHK1 cleavage induced by Etp treatment, however, PARP1 cleavage was slightly decreased. Consistent with this result, CASP3, CASP7, and CASP9 activation in ETP-treated cells was slightly inhibited by co-treatment with AEBSF (data not shown). These results suggest that serine protease family proteins are also involved in CHK1 cleavage in PCD. The most well-characterized serine protease is HTRA2, which enhances apoptotic cell death via interaction with the endogenous apoptosis inhibitor XIAP, so we analyzed the involvement of HTRA2 in CHK1 cleavage by using a knockdown method (Fig. 1E). HTRA2 knockdown by siRNA slightly reduced Etp-induced CHK1 cleavage. To further support the involvement of HTRA2 in CHK1 cleavage, we sought to analyze the effect on CHK1 cleavage using Ucf-101, which is the best-known inhibitor of HTRA2 [23]. As shown in Fig. 1F, chemical inhibition of HTRA2 completely inhibited CHK1 cleavage. These results show that HTRA2 is one of the candidate serine proteases involved in the regulation of CHK1 cleavage.

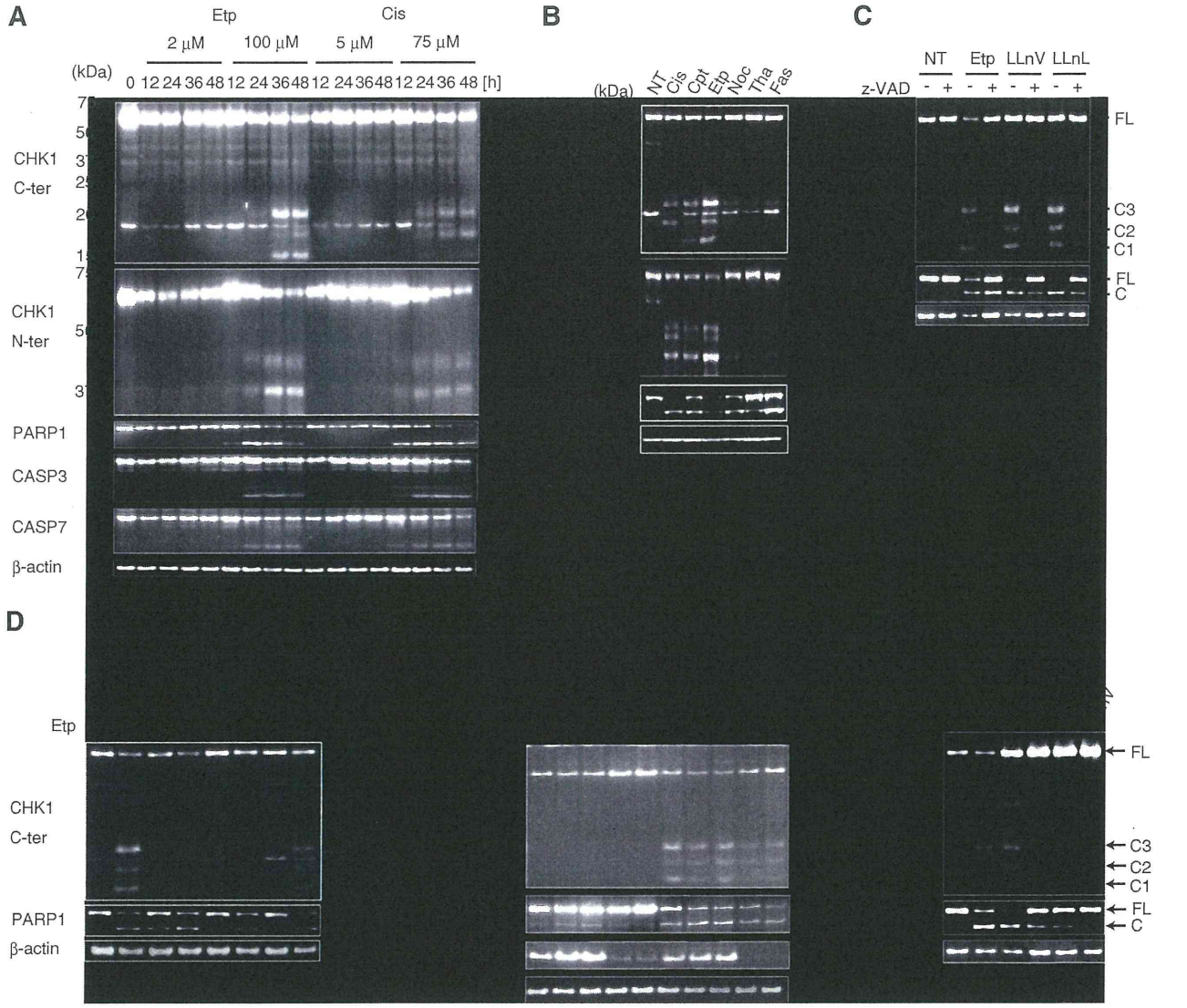

Fig. 1. Efficient CHK1 cleavage in DNA damage-induced PCD and the involvement of CASP and serine protease family. (A) U2OS cells were treated with the indicated doses of Etp or Cis for indicated times. The cell lysates were analyzed by Western blotting with the indicated antibodies. (B) U2OS cells treated with various apoptosis-inducing agents for 36 h were analyzed by Western blotting. NT, non-treatment; Cis, 60 μM Cis; Cpt, 20 μM Cpt; Etp, 100 μM Etp; Noc, 500 nM Noc; Tha, 2 μM Tha; FAS, 50 ng/mL anti-FAS (CH-11) and 20 μM Chx. (C) U2OS cells were pretreated in the absence or presence of 100 μM z-VAD-fmk for 1 h, and ETP, LLnV, or LLnL was then added into the medium at a final concentration of 100, 2, or 50 μM, respectively. After another 48-h incubation, the cells were harvested. The lysates were analyzed by Western blotting with the indicated antibodies. (D) U2OS cells were pretreated in the absence or presence of the indicated serine protease inhibitors (400 nM AEBSF, 300 nM TLCK, 80 nM TPCK) for 1 h, and ETP was then added into the medium at a final concentration of 100 μM. After another 48-h incubation, the cells were harvested. The lysates were analyzed by Western blotting with the indicated antibodies. The asterisk indicates a non-specific band. (E) siRNA transfected U2OS cells were treated with 100 μM ETP for 36 h. The lysates were analyzed by Western blotting with the indicated antibodies. Non-si: no siRNA, siScr: scramble siRNA, siHTRA2: HTRA2 siRNA. (F) U2OS cells were pretreated in the absence or presence of 50 μM Ucf-101 for 1 h, and ETP was then added into the medium at a final concentration of 100 μM. After another 48-h incubation, the cells were harvested. The lysates were analyzed by Western blotting with the indicated antibodies.

3.2. Identification of CASP family proteases responsible for CHK1 cleavage and the effect of cleavage on CHK1 kinase activity

As shown in Fig. 1, since all CHK1 cleavages in PCD were regulated in a CASP-dependent manner, we predicted that CASP family proteases directly catalyze CHK1 cleavage. Hence, we performed CHK1 cleavage assays using recombinant CASP2, CASP3, CASP6, CASP7, CASP8, CASP9, or CASP10, which are categorized as apoptotic CASPs [3–5]. Recombinant CHK1 was prepared as a protein fused with 3× FLAG tag at its N-terminus and 3× Myc tag at its C-terminus. The C-terminal products of CHK1 were detected by Western blotting using anti-Myc. The results showed that CHK1 is cleaved into two major products by CASP3 or CASP7 (Fig. 2A). Considering the molecular weights of cleavage products shown in Fig. 1, it was considered likely that the two major signals were from C3 (probably due to cleavage at D^{299}) and C1 (probably due to cleavage at D^{351}) fragments. A comparison to mobility of CHK1 cleavage fragments from the positive control (Etp-treated cell lysate expressing 3× FLAG-CHK1–3× Myc) supported this estimation (Supplemental Fig. II). To ensure that the two major products were from D^{299} and D^{351}, we examined whether a D299E or D351E mutation inhibits CASP3 or CASP7-mediated CHK1 cleavage. In D299E and D351E mutants, we detected only C3 and C1 fragments, respectively (Fig. 2B). This result demonstrates that C3 and C1 fragments are derived from cleavage at D^{299} and D^{351}, respectively. Furthermore, to aid prediction of the in vivo contribution of CASP3 and CASP7, we tested whether

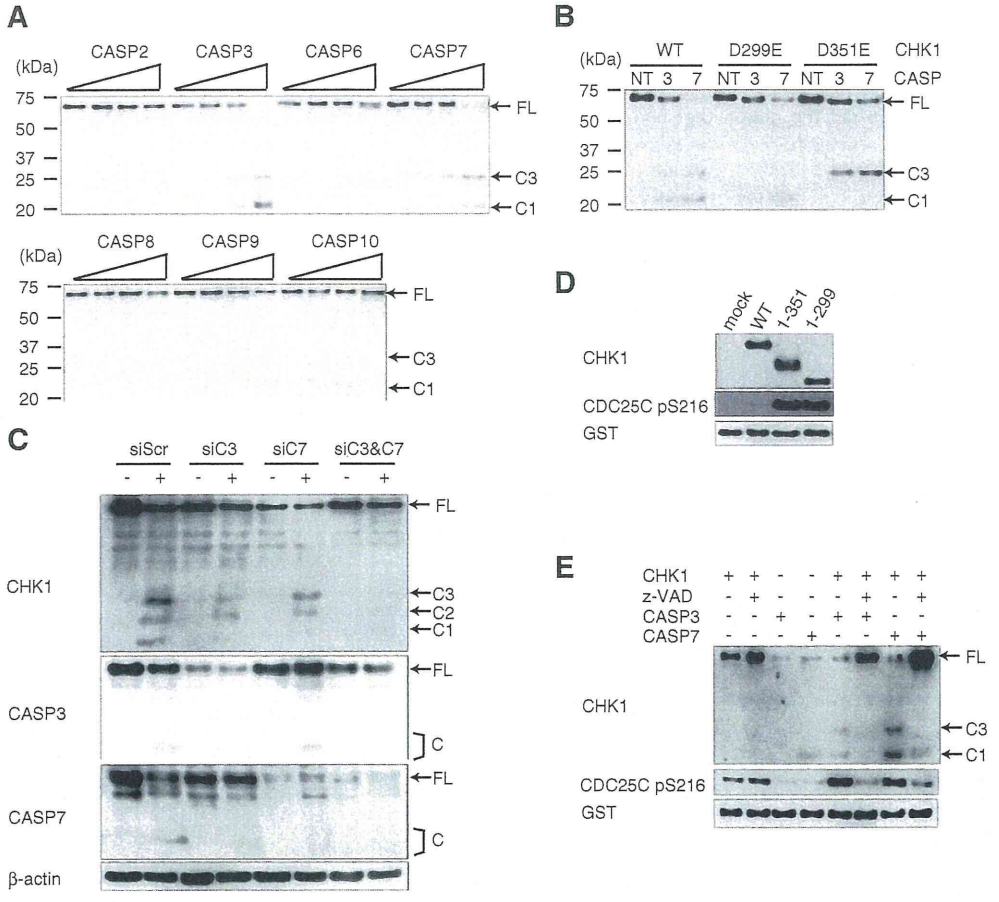

Fig. 2. Identification of CASP family proteases responsible for CHK1 cleavage and the effect of cleavage on CHK1 kinase activity. (A) Recombinant 3× FLAG-CHK1–3× Myc was incubated with apoptosis-related CASP2, CASP3, CASP6, CASP7, CASP8, CASP9, or CASP10 for 24 h at 37 °C. CHK1 cleavage was analyzed by western blotting using anti-Myc-Tag antibody. (B) Recombinant 3× FLAG-CHK1–3× Myc (CHK1 WT, D299E or D351) was incubated with CASP3 or CASP7 for 24 h at 37 °C. CHK1 cleavage was analyzed by western blotting using anti-Myc-Tag antibody. (C) U2OS cells were transfected with 10 nM siRNAs against GFP (siScr), CASP3 (siC3), CASP7 (siC7), or siC3 and siC7 for 24 h, and then treated with 100 μM ETP for 48 h. CHK1 cleavage was analyzed by western blotting using the indicated antibodies. (D) In vitro translated full-length CHK1 (WT) or truncated forms of CHK1(1–299, 1–351) were incubated with GST-CDC25C at 30 °C for 30 min. CHK1 kinase activity was analyzed by Western blotting with anti-CDC25C (pSer216). (E) Recombinant CHK1 was pre-incubated with or without CASP3, CASP7, at 37 °C for 8 h in the presence or absence of 100 μM zVAD-fmk. CHK1 was then incubated with GST-CDC25C at 30 °C for 30 min, and analyzed by Western blotting with the indicated antibodies.

siRNA-mediated knockdown of CASP3 or CASP7 inhibits CHK1 cleavage in DNA damage-induced PCD. As shown in Fig. 2C, knockdown of CASP3, CASP7, or both CASP3 and CASP7 inhibited CHK1 cleavage. These results show that CASP3 and CASP7 are responsible for CHK1 cleavage at both D^{299} and D^{351}.

We subsequently performed CHK1 kinase assays to evaluate cleaved CHK1 kinase activity. Since CHK1 has an auto-inhibitory region at its C-terminus [24–27], we estimated that CHK1 cleavage has the potential to elevate its kinase activity. In this study, we used an assay that detects CDC25C phosphorylation by Western blotting with an anti-CDC25C(phospho-S^{216}) probe [18]. We first prepared full-length, CHK1(FL), and cleavage forms of CHK1 containing the relevant kinase domain, CHK1(1–299) and CHK1(1–351). As shown in Fig. 2D, kinase activities of both CHK1(1–299) and CHK1(1–351) drastically increased in comparison to that of CHK1(FL). This observation is consistent with past studies that found that deletion of the C-terminus of CHK1 enhances its kinase activity [15,24–27]. Next, we tested whether the activity of the CASP-cleaved CHK1 containing the kinase domain fragment and auto-inhibitory region was elevated. Recombinant CHK1(FL) pre-incubated with or without CASP3 or CASP7 in the presence or absence of 100 μM zVAD-fmk was subjected to the CHK1 kinase assay (Fig. 2E). The kinase activity of CHK1 pre-incubated with CASP3 or CASP7 was elevated in comparison to that of pre-incubated CHK1 alone, and the elevation was inhibited by co-pretreatment with z-VAD. These results show that the cleavage of CHK1 by CASP3 or CASP7 elevates its kinase activity.

3.3. *Identification of a recognition sequence associated with non-CASP family proteases in CHK1 cleavage*

From the results of Fig. 2A, we noticed that none of the apoptotic CASP proteases induced production of a C2 fragment. Since this result raised the possibility that non-CASP family proteases are involved in N2–C2 cleavage, we performed further analyses of the recognition sequence. Previously, it has been reported that the P1 residue in the CASP recognition sequence is an aspartic acid residue [3–5]. This implies that if N2–C2 cleavage is catalyzed by the CASP family, a mutation of the P1 residue would result in inhibition of cleavage. Therefore, we sought to identify the recognition sequence of N2–C2 cleavage by using site-directed mutagenesis involving mutation of aspartic acid to glutamic acid. Considering the molecular weights of the cleavage products (Fig. 1), we explored aspartic acid residues in the surrounding amino acid sequences and found aspartic acid residues at positions 258, 262, 299, 329, 336, 351, 385, and 387 (Fig. 3A). Next, we constructed plasmid vectors harboring a wild-type or an aspartic acid-to-glutamic acid substitution mutant of CHK1 with a Flag-tag at the N-terminus and a Myc-tag at the C-terminus. After induction of PCD in U2OS cells that had been

transfected with each vector, the C-terminal fragments of CHK1 were analyzed by Western blotting with anti-Myc (Fig. 3B). Although D299E and D351E mutation inhibited production of C3 and C1, respectively, we could not identify any mutation that inhibited production of C2. This result supported the notion that non-CASP family proteases are involved in N2–C2 cleavage. Next, to identify the recognition sequence associated with the non-CASP family proteases (termed as seq-X), we devised a strategy to narrow down the identification of seq-X by using C- or N-terminal deletion mutants (Fig. 3C). Firstly, for detection of cleaved products, C-terminal and N-terminal

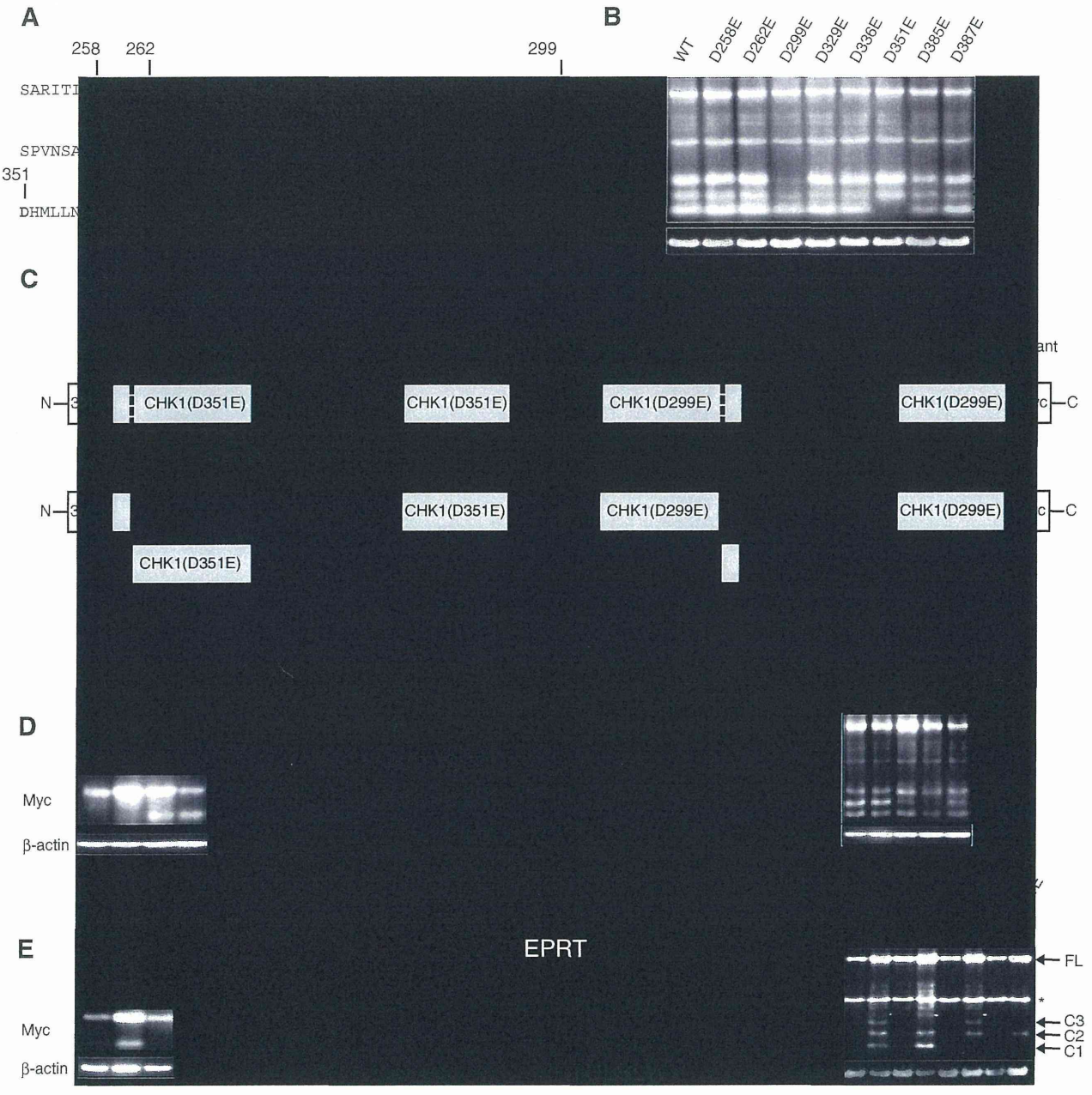

Fig. 3. Identification of a recognition sequence associated with non-CASP family proteases in CHK1 cleavage. (A) CHK1 amino acid sequences between position 251 and position 410 are shown. Bold letters represent aspartic acid residues. (B) A plasmid vector harboring a wild-type CHK1 or a glutamic acid substitution CHK1 mutant form of D^{258}, D^{262}, D^{299}, D^{329}, D^{336}, D^{351}, D^{385}, or D^{387} was transfected into U2OS cells. The cells were treated with 100 μM Etp for 36 h, and the cleaved C-terminal fragments of CHK1s were analyzed by Western blotting with anti-Myc. The asterisk indicates a non-specific band. (C) Strategy for identification of recognition sequences for cleavage at seq-X. N-terminal and C-terminal deletion mutants were fused to 3× Myc at the N-terminal and C-terminal, respectively. For cleavage at only seq-X, D^{299} in each C-terminal deletion mutant and D^{351} in each N-terminal deletion mutant were mutated to alanine. After PCD induction, only mutants possessing the recognition sequences were cleaved into two fragments as shown. (D and E) U2OS cells were transfected with expression vectors encoding the indicated N-terminal (D) or C-terminal (E) deletion mutants. After 36 h of transfection, the cells were treated with 100 μM Etp for 48 h. (F) The recognition sequences for cleavage at seq-X were estimated from the data presented in panels D and E. The asterisk indicates a non-specific band. (G) A plasmid vector harboring a wild-type CHK1 or an alanine substitution CHK1 mutant form of E^{320}, P^{321}, R^{322}, or T^{323} was transfected into U2OS cells. The cells were treated with 100 μM Etp for 36 h, and the C-terminal fragments of CHK1s were analyzed by Western blotting with anti-Myc. (H) A plasmid vector harboring a wild-type CHK1 or a glutamic acid substitution CHK1 mutant form of D^{299}, D^{351}, or D^{299} and D^{351} was transfected into U2OS cells. The cells were treated with 2 μM LLnV for 36 h, and the cleaved C-terminal fragments of CHK1s were analyzed by Western blotting with anti-Myc. The asterisk indicates a non-specific band.

deletion mutants were fused to 3× Myc at the C-terminus and N-terminus, respectively. Secondly, for detection of products cleaved at only seq-X but not other identified sequences, D^{299} in each C-terminal deletion mutant and D^{351} in each N-terminal deletion mutant were mutated to glutamic acid. By this strategy, it is likely that after PCD induction, only mutants possessing seq-X are cleaved into two fragments and the smaller products fused to 3× Myc tag are detected by Western blotting with anti-Myc antibody. Because preliminary analyses using N-terminal deletion mutants (311–476, 316–476, and 321–476 mutants) and C-terminal deletion mutants (1–318, 1–320, 1–322, and 1–324 mutants) suggested that the putative seq-X is located between positions 319 and 324 (data not shown), we further analyzed using four C-terminal deletion mutants (1–321, 1–322, 1–323, and 1–324) and three N-terminal deletion mutants (319–476, 320–476, and 321–476). As shown in Fig. 3D, in N-terminal deletion series, the 321–476 mutant was not cleaved. As shown in Fig. 3E, In the C-terminal deletion series, the 1–321 and 1–322 mutants were not cleaved. These results show that the seq-X is ^{320}EPRT^{323} or, in other words, that it is not a CASP consensus sequence (Fig. 3F), suggesting that the "EPRT proteases" in question are non-CASP family proteases. Furthermore, we confirmed whether alanine mutations of these sequences affect cleavage. As shown in Fig. 3G, P321A and R322A mutation, but not E320A and T323A mutation, efficiently inhibited production of the C2 fragment. Moreover, the inhibition of EPRT cleavage by site-directed mutagenesis did not affect either D^{299} or D^{351} cleavage. We also analyzed whether the mutation of sites cleaved by CASP affect EPRT cleavage (Fig. 3H). The mutation of D^{299} and/or D^{351} cleavage did not significantly affect EPRT cleavage. Taken together, these results indicate that CHK1 cleavage by CASP and non-CASP can occur independently of each other.

3.4. PCD induction at a specific cell cycle phase and CHK1 cleavage

Considering that CHK1 is involved in cell cycle regulation, we explored the relationship between PCD at a specific cell cycle phase and CHK1 cleavage, using DNA damaging agents. We chose to use Cis, a direct DNA crosslinker as a PCD inducer. Indirect DNA damaging agents such as Cpt and Etp, for example, were not appropriate for our purposes, because their pharmacological effects are dependent on cell cycle phases. First, using the DTB method, G1/S-boundary, S, G2, or G1 phase-enriched cells were prepared and then induced to PCD by treatment with Cis (Fig. 4A). PCD induction of G1 phase-enriched cells induced a CHK1 cleavage profile that was different to the profiles induced by PCD induction of cells enriched from the other phases. The cleavage products (both N- and C-terminus) from ^{320}EPRT^{323} markedly increased compared with those from D^{299} and D^{351} (Fig. 4B). Using a marker of apoptosis, PARP1 cleavage, it was apparent that the induction efficiency of PCD in G1/S or G1 phase-enriched cells was higher than that of S and G2 phase-enriched cells. To exclude the possibility that these findings result from an artifact of the DTB method, we confirmed the finding by using cells synchronized by the TNB method. By this method, M, G1, or S phase-enriched cells were prepared and then treated with Cis to induce PCD (Fig. 4C). As shown in Fig. 4D, PCD induction of cells enriched from G1 phase, but not M and S phases, caused increased cleavage at ^{320}EPRT^{323}. Furthermore, from the results of PARP1 cleavage and CASP3 activation, the efficiency of PCD induction in M or G1 phase-enriched cells was higher than that of S phase-enriched cells. These results indicate that CHK1 cleavage, when inducing PCD at G1 phase, is different from that of the other phases.

4. Discussion

In this study, we showed the intricate regulatory mechanisms of CHK1 cleavage during PCD (Fig. 5). Firstly, we showed that CHK1 cleavage efficiently occurs in PCD induced by DNA damaging agents such as Cis, Cpt, and Etp, as well as cathepsin, calpain, and proteasome inhibitors such as LLnV and LLnL (Fig. 1B and 1C). DNA damage-induced PCD led to increases in protein levels of cleaved CHK1 and decreases in protein levels of full-length CHK1. On the other hand, LLnV and LLnL-induced PCD led to increases in protein levels of cleaved CHK1 without any significant decrease in full-length CHK1. Considering that ubiquitin–proteasome pathway is involved in turnover of CHK1 protein [28–30], the increases of total CHK1 protein may spoil the decreases in the protein levels of full-length CHK1 induced by PCD. Next, we showed that both CASP and a specific serine protease family regulate CHK1 cleavage. Interestingly, serine protease inhibitors efficiently inhibited CHK1 cleavage and slightly inhibited PARP1 cleavage (Fig. 1D). Considering that PARP1 is cleaved by CASP3 and CASP7 as well as CHK1 [31,32], these results means that although the CASP3 or CASP7-mediated PCD pathway were still active, CHK1 cleavage was completely inhibited. Hence, CASPs activation is essential but not sufficient for CHK1 cleavage. It may be that the serine proteases are required for changing CHK1 to a "cleavable state" (for example, elimination of endogenous CHK1 cleavage inhibitor) rather than cleaving CHK1 directly. In any case, our results indicate that even if PCD is CASP independent, CASP activation would be required for CHK1 cleavage. Furthermore, we demonstrated that one candidate serine protease involved in CHK1 cleavage is HTRA2. It is known that HTRA2 enhances both CASP-dependent and CASP-independent PCD pathways [33]. Consistent with this result, serine protease inhibitor treatment slightly inhibited the activation of some apoptotic CASPs in DNA damage-induced PCD (data not shown). Considering that CASP3 and CASP7 are activated even under serine protease inhibition, HTRA2 may contribute to CHK1 cleavage in a CASP-independent manner. Interestingly, we noticed that even in the absence of Etp or LLnV treatment, HTRA2 inhibition by siRNA-mediated gene knockdown or chemical inhibition elevated the CHK1 protein levels (Fig. 1E and F). This result may imply the physiological interaction between HTRA2 and CHK1. To address whether only HTRA2 contributes to CHK1 cleavage as the serine protease, HTRA2 deficient cells would be required.

Our results suggest that CHK1 cleavage is directly executed by CASP3, CASP7, and as yet unidentified non-CASP family proteases, and that CHK1 cleavage by CASP and non-CASP can occur independently of each other (Figs. 2 and 3). As shown in Fig. 2A, we obtained in vitro data that both CASP3 and CASP7 cleave CHK1 at both D^{299} and D^{351}, and none of the apoptotic CASPs cleave CHK1 by recognizing ^{320}EPRT^{323}(Fig. 3C–G). Taken together with the fact that EPRT is not a CASP consensus recognition sequence, our results strongly suggest that the unidentified protease is not a member of the CASP family. While the truncation analysis suggests that ^{320}EPRT^{323} is the recognition sequence, P321A and R322A mutation, but not E320A and T323A mutation, efficiently inhibited ^{320}EPRT^{323} cleavage (Fig. 3C–G). Hence, mutation analyses other than Ala would be required to determine the essential amino acid residue(s) in the ^{320}EPRT^{323} cleavage. We suspected the involvement of lysosomal proteases such as the cathepsin family in ^{320}EPRT^{323} cleavage, because lysosomes are reportedly involved in apoptotic cell death [34]. The inhibition of Cathepsin B, D, G, or L by chemical compounds [34–37], which are involved in certain types of PCD [38], did not inhibit all instances of CHK1 cleavage (data not shown). In addition, the inhibition of pH-dependent lysosomal proteases by bafilomycin A1 [35] did not affect CHK1 cleavages (data not shown). These results indicate that proteases other than those described above would contribute to CHK1 cleavages. Moreover, we obtained data that, under conditions whereby calpains, cathepsins, and proteasomes are inhibited, CHK1 cleavage can occur (Fig. 1C). The fact that siRNA-mediated knockdown of CASP3 and/or CASP7, and z-VAD-fmk treatment, inhibit EPRT cleavage suggests that EPRT protease(s) is also regulated by the CASP pathway (Fig. 2C). We are currently exploring candidate proteases of ^{320}EPRT^{323} cleavage. Furthermore, in the induction of PCD in cell cycle-synchronized cells, we obtained the interesting

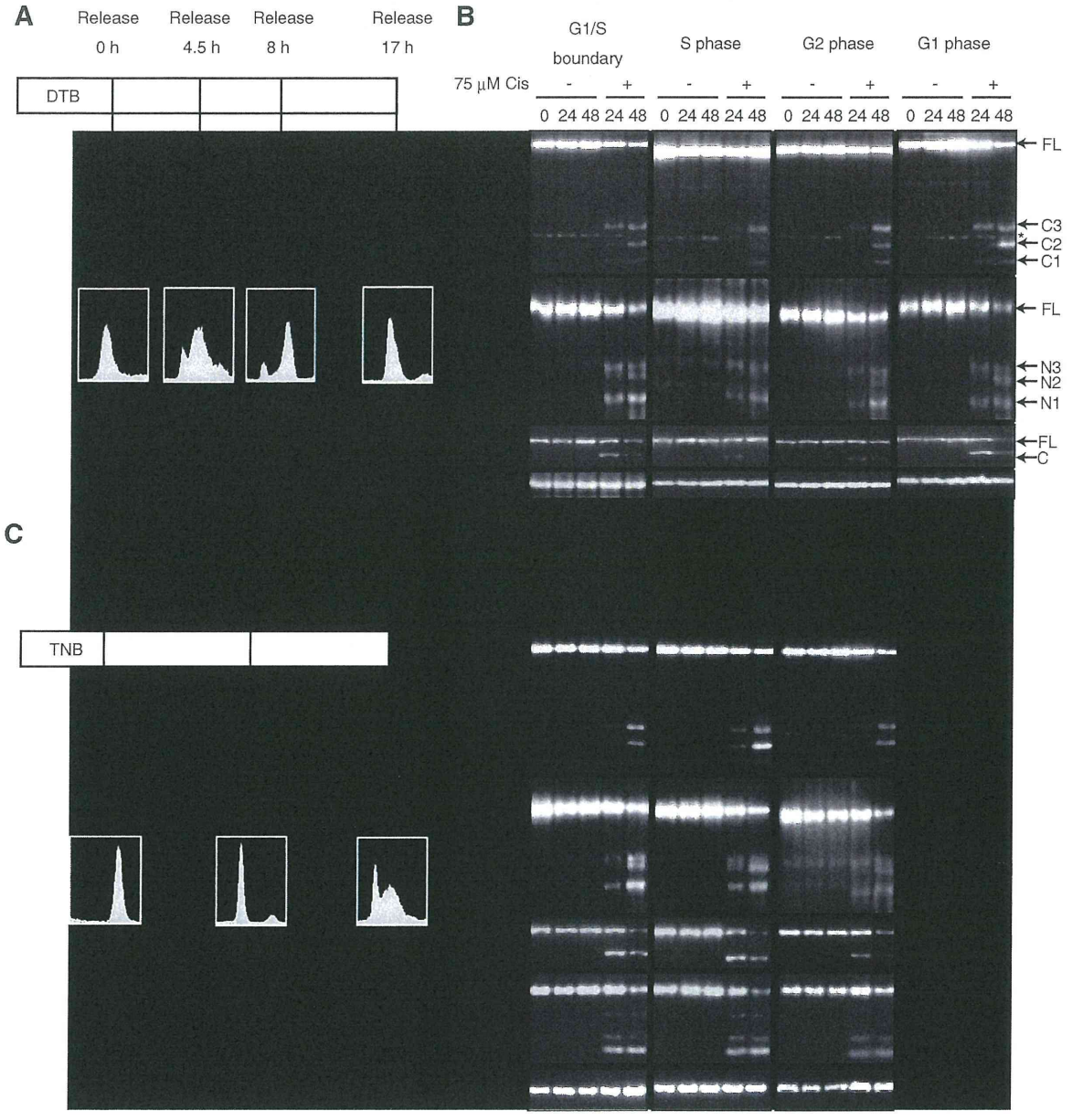

Fig. 4. Enhancement of CHK1 cleavage by EPRT protease in PCD induction at a specific cell cycle phases. (A and C) Procedures for analysis of the cell cycle specificity of CHK1 cleavage. (B) U2OS cells synchronized at G1, G1/S, S, or G2 phase by DTB method were treated with 75 μM of Cis and the cell extracts were analyzed by Western blotting with the indicated antibodies. (D) U2OS cells synchronized at M, G1, or S (right) phase by TNB methods were treated with 75 μM of Cis and the cell extracts were analyzed by Western blotting with the indicated antibodies. The asterisk indicates a non-specific band.

observation that ^{320}EPRT^{323} cleavage of CHK1 occurs efficiently in PCD, which is induced at the G1 phase (Fig. 4). On the other hand, we did not observe a cell cycle phase preference for D^{299} and D^{351} cleavage. We suggest two possibilities that may explain this cell cycle-related difference in ^{320}EPRT^{323} cleavage. The first possibility is that EPRT proteases may be activated and/or up-regulated at G1 phase. Currently, we do not know any PCD-related proteases that are regulated in a cell cycle phase-specific manner. However, considering the existence of cell cycle-selective PCD such as mitotic catastrophe [1,2], such proteases may exist. The second possibility is that post-transcriptional modification of CHK1 may increase the efficiency of ^{320}EPRT^{323} cleavage. A previous study has reported that cleavage-site phosphorylation is disadvantageous with respect to cleavability by CASPs [39]. We are interested in the relationship between post-transcriptional modifications of CHK1 and effects on CHK1 cleavage. Our group and another have already confirmed that S^{317} and S^{345} phosphorylations, which are well known as DNA damage-responsive phosphorylation sites, do not critically affect CHK1 cleavage during PCD (data not shown, 15). Furthermore, in PCD in G1 phase-enriched cells, since the CASP-cleaved sites D^{299} and D^{35} are also cleaved, the physiological significance appears to not be simple as the EPRT cleavage compensates for D^{299} and/or D^{351} cleavage. It remains unclear whether the preferential cleavage of ^{320}EPRT^{323} at G1 phase contributes to the regulation of cell cycle-selective PCD, directly or indirectly.

We found that CHK1 cleavage leads to elevated kinase activity (Fig. 2D and E). Although the data presented here indicate that CASP3 and CASP7-mediated cleavage elevates CHK1 kinase activity, we were not able to address the effect on kinase activity by ^{320}EPRT^{323} protease-mediated cleavage because the position of amide bonds cleaved by ^{320}EPRT^{323} proteases has been not identified. Nevertheless,

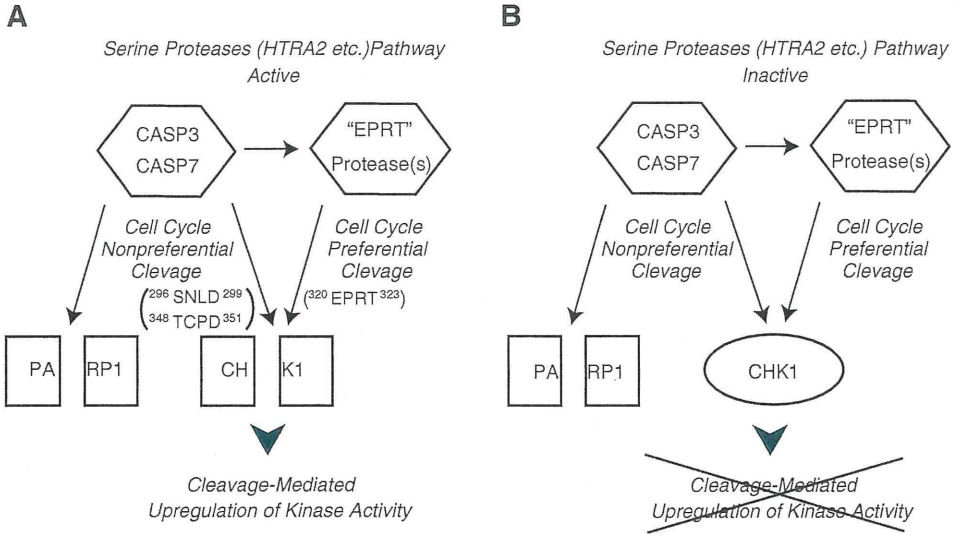

Fig. 5. A model of CHK1 cleavage regulation during PCD. The PCD signal activates certain types of serine proteases such as HTRA2 as well as the CASP family. The serine protease(s)-involved pathway alters CHK1 to the cleavable state. Therefore, under conditions where the serine protease(s) is active, CHK1 is cleaved by CASP3 and CASP7 at ^{296}SNLD^{299} and ^{348}351 in a cell cycle-nonpreferential manner, and by unidentified EPRT proteases at ^{320}EPRT^{323} in a cell cycle-preferential manner, which results in elevated kinase activity (A). On the other hand, under conditions where the serine protease(s) is inactive, CHK1 is not cleaved (B). PARP1 is cleaved by CASP3 and CASP7 without critical involvement of the serine protease pathway.

we anticipate that CHK1 cleavage by ^{320}EPRT^{323} proteases would induce up-regulation of its kinase activity as well as that by CASPs. The basis for this prediction is as follows: i) The auto-inhibitory region of CHK1 is located at approximately 100 amino acids from its C-terminus (full-length CHK1; 476 amino acids) [24–27], ii) ^{320}EPRT^{323} lies between ^{296}SNLD^{299} and ^{348}TCPD^{351} (Fig. 3), iii) the kinase activity of CHK1(1–299) and CHK1(1–351) increases compared with that of full-length CHK1 (Fig. 2), and iv) the kinase activity of CHK1(1–308) and CHK1(1–335) increases compared with that of full-length CHK1 [26]. The most important question is how PCD-specific CHK1 activation affects PCD. The regulation of CHK1 cleavage may be a secondary event in PCD because, as shown in Fig. 2, CHK1 cleavage requires CASP3 and CASP7 activation, which generally occur after loss of mitochondrial membrane potential [1,2]. Considering that CHK1 inhibits cell cycle progression in response to DNA damage, cell cycle progression should already be arrested prior to the execution of DNA damage-induced PCD. Therefore the cleavage-mediated CHK1 activation may contribute to shutdown the cell cycle machinery or to afford more efficient processing of cellular components during PCD. To clarify this question would require investigation of the differences of binding partners or substrate specificity between full-length CHK1 and cleaved CHK1.

It has been reported that previously identified "death substrates involved in DNA damage response" are cleaved or regulated by CASP [7–13]. On the other hand, CHK1 cleavage is involved in multiple protease families (serine protease, CASP, and unidentified EPRT protease family). These findings may imply that CHK1 cleavage plays an important role in DNA damage-induced PCD, or that "death substrate cleavage" itself may involve more complicated mechanisms than previously thought. In any case, the contribution of CHK1 cleavage to PCD is not likely to be simple. To study the contribution of CHK1 cleavage to PCD via these intricate regulatory mechanisms, requires not only the identification of proteases involved in CHK cleavage but also lethality and the processes of various types of PCD. Furthermore to clarify the physiological roles of CHK1 cleavage, requires evaluation of whether the inhibition of all CHK1 cleavages and subsequent changes of kinase activity affect PCD. We are constructing cells that stably express mutants that are kinase active and uncleavable and kinase inactive and uncleavable. By using these cells, we will evaluate the effects of CHK1 cleavage on PCD by coordinating various viewpoints such as ATP/NAD$^+$ levels, chromatin condensation, mitochondrial outer membrane potential, membrane blebbing, and so on. In summary, our results shed light on the complexity of PCD-mediated protein cleavage and cell cycle-specific regulation of the PCD pathway. CHK1 cleavage may provide a useful model to show the complexity involved in this regulation.

Supplementary data to this article can be found online at http://dx.doi.org/10.1016/j.bbagen.2012.10.009.

Acknowledgements

We thank Dr. Jun-ichi Sakai, Mr. Akihiko Mizoroki, Mr. Toru Sakagami, and Ms. Kikumi Yoshida (Tokyo University of Science, Japan) for their technical assistance; and all members of Tanuma and Higami laboratories for their cooperation. The first author also thanks Machiko Okita and Soju Okita for their valuable encouragement. This work was supported by a Research Grant for Promoting Technological Seeds (A) from the Japan Science and Technology Agency (N.O.) and a Research Grant for Young Scientists from Tokyo University of Science (N.O.) and partially by a Grant-in-Aid for Young Scientists (B) (23790201) from the Ministry of Education, Culture, Sports, Science and Technology (N.O.).

References

[1] G. Kroemer, L. Galluzzi, P. Vandenabeele, J. Abrams, E.S. Alnemri, E.H. Baehrecke, M.V. Blagosklonny, W.S. El-Deiry, P. Golstein, D.R. Green, M. Hengartner, R.A. Knight, S. Kumar, S.A. Lipton, W. Malorni, G. Nuñez, M.E. Peter, J. Tschopp, J. Yuan, M. Piacentini, B. Zhivotovsky, G. Melino, Classification of cell death: recommendations of the Nomenclature Committee on Cell Death 2009, Cell Death Differ. 16 (2009) 3–11.

[2] L. Galluzzi, I. Vitale, J.M. Abrams, E.S. Alnemri, E.H. Baehrecke, M.V. Blagosklonny, T.M. Dawson, V.L. Dawson, W.S. El-Deiry, S. Fulda, E. Gottlieb, D.R. Green, M.O. Hengartner, O. Kepp, R.A. Knight, S. Kumar, S.A. Lipton, X. Lu, F. Madeo, W. Malorni, P. Mehlen, G. Nuñez, M.E. Peter, M. Piacentini, D.C. Rubinsztein, Y. Shi, H.U. Simon, P. Vandenabeele, E. White, J. Yuan, B. Zhivotovsky, G. Melino, G. Kroemer, Molecular definitions of cell death subroutines: recommendations of the Nomenclature Committee on Cell Death 2012, Cell Death Differ. 19 (2012) 107–120.

[3] R.V. Talanian, C. Quinlan, S. Trautz, M.C. Hackett, J.A. Mankovich, D. Banach, T. Ghayur, K.D. Brady, W.W. Wong, Substrate specificities of caspase family proteases, J. Biol. Chem. 272 (1997) 9677–9682.

[4] N.A. Thornberry, T.A. Rano, E.P. Peterson, D.M. Rasper, T. Timkey, M. Garcia-Calvo, V.M. Houtzager, P.A. Nordstrom, S. Roy, J.P. Vaillancourt, K.T. Chapman, D.W. Nicholson, A combinatorial approach defines specificities of members of the caspase family and granzyme B. Functional relationships established for key mediators of apoptosis, J. Biol. Chem. 272 (1997) 17907–17911.

[5] C. Pop, G.S. Salvesen, Human caspases: activation, specificity, and regulation, J. Biol. Chem. 284 (2009) 21777–21781.
[6] K. Schrader, J. Huai, L. Jöckel, C. Oberle, C. Borner, Non-caspase proteases: triggers or amplifiers of apoptosis? Cell. Mol. Life Sci. 67 (2010) 1607–1618.
[7] Y.A. Lazebnik, S.H. Kaufmann, S. Desnoyers, G.G. Poirier, W.C. Earnshaw, Cleavage of poly(ADP-ribose) polymerase by a proteinase with properties like ICE, Nature 371 (1994) 346–347.
[8] Y. Huang, S. Nakada, T. Ishiko, T. Utsugisawa, R. Datta, S. Kharbanda, K. Yoshida, R.V. Talanian, R. Weichselbaum, D. Kufe, Z.M. Yuan, Role for caspase-mediated cleavage of Rad51 in induction of apoptosis by DNA damage, Mol. Cell. Biol. 19 (1999) 2986–2997.
[9] G.C. Smith, F. d'Adda di Fagagna, N.D. Lakin, S.P. Jackson, Cleavage and inactivation of ATM during apoptosis, Mol. Cell. Biol. 19 (1999) 6076–6084.
[10] M.W. Lee, I. Hirai, H.G. Wang, Caspase-3-mediated cleavage of Rad9 during apoptosis, Oncogene 22 (2003) 6340–6346.
[11] C.A. Clarke, L.N. Bennett, P.R. Clarke, Cleavage of claspin by caspase-7 during apoptosis inhibits the Chk1 pathway, J. Biol. Chem. 280 (2005) 35337–35345.
[12] N. Okita, Y. Kudo, S. Tanuma, Checkpoint kinase 1 is cleaved in a caspase-dependent pathway during genotoxic stress-induced apoptosis, Biol. Pharm. Bull. 30 (2007) 359–362.
[13] S. Solier, Y. Pommier, MDC1 cleavage by caspase-3: a novel mechanism for inactivating the DNA damage response during apoptosis, Cancer Res. 71 (2011) 906–913.
[14] S. Mansilla, W. Priebe, J. Portugal, Mitotic catastrophe results in cell death by caspase-dependent and caspase-independent mechanisms, Cell Cycle 5 (2006) 53–60.
[15] K. Matsuura, M. Wakasugi, K. Yamashita, T. Matsunaga, Cleavage-mediated activation of Chk1 during apoptosis, J. Biol. Chem. 283 (2008) 25485–25491.
[16] S. Sidi, T. Sanda, R.D. Kennedy, A.T. Hagen, C.A. Jette, R. Hoffmans, J. Pascual, S. Imamura, S. Kishi, J.F. Amatruda, J.P. Kanki, D.R. Green, A.A. D'Andrea, A.T. Look, Chk1 suppresses a caspase-2 apoptotic response to DNA damage that bypasses p53, Bcl-2, and caspase-3, Cell 133 (2008) 864–877.
[17] K. Myers, M.E. Gagou, P. Zuazua-Villar, R. Rodriguez, M. Meuth, ATR and Chk1 suppress a caspase-3-dependent apoptotic response following DNA replication stress, PLoS Genet. 5 (2009) e1000324.
[18] Y.S. Kaneko, N. Watanabe, H. Morisaki, H. Akita, A. Fujimoto, K. Tominaga, M. Terasawa, A. Tachibana, K. Ikeda, M. Nakanishi, Cell-cycle-dependent and ATM-independent expression of human Chk1 kinase, Oncogene 18 (1999) 3673–3681.
[19] K.L. Rock, C. Gramm, L. Rothstein, K. Clark, R. Stein, L. Dick, D. Hwang, A.L. Goldberg, Inhibitors of the proteasome block the degradation of most cell proteins and the generation of peptides presented on MHC class I molecules, Cell 78 (1994) 761–771.
[20] P. Vandenabeele, S. Orrenius, B. Zhivotovsky, Serine proteases and calpains fulfill important supporting roles in the apoptotic tragedy of the cellular opera, Cell Death Differ. 12 (2005) 1219–1224.
[21] H.J. Rideout, E. Zang, M. Yeasmin, R. Gordon, O. Jabado, D.S. Park, L. Stefanis, Inhibitors of trypsin-like serine proteases prevent DNA damage-induced neuronal death by acting upstream of the mitochondrial checkpoint and of p53 induction, Neuroscience 107 (2001) 339–352.
[22] E.C. de Bruin, D. Meersma, J. de Wilde, I. den Otter, E.M. Schipper, J.P. Medema, L.T. Peltenburg, A serine protease is involved in the initiation of DNA damage-induced apoptosis, Cell Death Differ. 10 (2003) 1204–1212.
[23] L. Cilenti, Y. Lee, S. Hess, S. Srinivasula, K.M. Park, D. Junqueira, H. Davis, J.V. Bonventre, E.S. Alnemri, A.S. Zervos, Characterization of a novel and specific inhibitor for the pro-apoptotic protease Omi/HtrA2, J. Biol. Chem. 278 (2003) 11489–11494.
[24] P. Chen, C. Luo, Y. Deng, K. Ryan, J. Register, S. Margosiak, A. Tempczyk-Russell, B. Nguyen, P. Myers, K. Lundgren, C.C. Kan, P.M. O'Connor, The 1.7 A crystal structure of human cell cycle checkpoint kinase Chk1: implications for Chk1 regulation, Cell 100 (2000) 681–692.
[25] Y. Katsuragi, N. Sagata, Regulation of Chk1 kinase by autoinhibition and ATR-mediated phosphorylation, Mol. Biol. Cell 15 (2004) 1680–1689.
[26] C.P. Ng, H.C. Lee, C.W. Ho, T. Arooz, W.Y. Siu, A. Lau, R.Y. Poon, Differential mode of regulation of the checkpoint kinases CHK1 and CHK2 by their regulatory domains, J. Biol. Chem. 279 (2004) 8808–8819.
[27] M. Walker, E.J. Black, V. Oehler, D.A. Gillespie, M.T. Scott, Chk1 C-terminal regulatory phosphorylation mediates checkpoint activation by de-repression of Chk1 catalytic activity, Oncogene 28 (2009) 2314–2323.
[28] Y.W. Zhang, D.M. Otterness, G.G. Chiang, W. Xie, Y.C. Liu, F. Mercurio, R.T. Abraham, Genotoxic stress targets human Chk1 for degradation by the ubiquitin-proteasome pathway, Mol. Cell 19 (2005) 607–618.
[29] V. Leung-Pineda, J. Huh, H. Piwnica-Worms, DDB1 targets Chk1 to the Cul4 E3 ligase complex in normal cycling cells and in cells experiencing replication stress, Cancer Res. 69 (2009) 2630–2637.
[30] Y.W. Zhang, J. Brognard, C. Coughlin, Z. You, M. Dolled-Filhart, A. Aslanian, G. Manning, R.T. Abraham, T. Hunter, The F box protein Fbx6 regulates Chk1 stability and cellular sensitivity to replication stress, Mol. Cell 35 (2009) 442–453.
[31] M. Tewar, L.T. Quan, K. O'Rourke, S. Desnoyers, Z. Zeng, D.R. Beidler, G.G. Poirier, G.S. Salvesen, V.M. Dixit, Yama/CPP32 beta, a mammalian homolog of CED-3, is a CrmA-inhibitable protease that cleaves the death substrate poly(ADP-ribose) polymerase, Cell 81 (1995) 801–809.
[32] T. Fernandes-Alnemri, A. Takahashi, R. Armstrong, J. Krebs, L. Fritz, K.J. Tomaselli, L. Wang, Z. Yu, C.M. Croce, G.S. Salvesen, W.C. Earnshaw, G. Litwack, E.S. Alnemri, Mch3, a novel human apoptotic cysteine protease highly related to CPP32, Cancer Res. 55 (1995) 6045–6052.
[33] R. Hegde, S.M. Srinivasula, Z. Zhang, R. Wassell, R. Mukattash, L. Cilenti, G. DuBois, Y. Lazebnik, A.S. Zervos, T. Fernandes-Alnemri, E.S. Alnemri, Identification of Omi/HtrA2 as a mitochondrial apoptotic serine protease that disrupts inhibitor of apoptosis protein–caspase interaction, J. Biol. Chem. 277 (2002) 432–438.
[34] N. Katunuma, E. Kominami, Structure, properties, mechanisms, and assays of cysteine protease inhibitors: cystatins and E-64 derivatives, Methods Enzymol. 251 (1995) 382–397.
[35] K. Ishidoh, E. Kominami, Processing and activation of lysosomal proteinases, Biol. Chem. 383 (2002) 1827–1831.
[36] H. Umezawa, Structures and activities of protease inhibitors of microbial origin, Methods Enzymol. 45 (1976) 678–695.
[37] M.N. Greco, M.J. Hawkins, E.T. Powell, H.R. Almond HR Jr., T.W. Corcoran, L. de Garavilla, J.A. Kauffman, R. Recacha, D. Chattopadhyay, P. Andrade-Gordon, B.E. Maryanoff, Nonpeptide inhibitors of cathepsin G: optimization of a novel beta-ketophosphonic acid lead by structure-based drug design, J. Am. Chem. Soc. 124 (2002) 3810–3811.
[38] S. Conus, H.U. Simon, Cathepsins: key modulators of cell death and inflammatory responses, Biochem. Pharmacol. 76 (2008) 1374–1382.
[39] J. Tözsér, P. Bagossi, G. Zahuczky, S.I. Specht, E. Majerova, T.D. Copeland, Effect of caspase cleavage-site phosphorylation on proteolysis, Biochem. J. 372 (2003) 137–143.